Supplemental information

Title: Clinical and functional analyses of NUP98-rearranged AML reveal quiescence-associated cell states and IL3RA activation

Jun Nagai, Toshihiro Matsukawa, Masahiro Onozawa, Shota Yoshida, Tomoki Takahashi, Fumiaki Fujii, Daigo Hashimoto, Takanori Teshima

Annals of Hematology

Corresponding author:
Toshihiro Matsukawa, MD, PhD
Department of Hematology, Hokkaido University Faculty of Medicine, Graduate School of Medicine, Sapporo, Japan
Kita 15, Nishi 7, Kita-ku, Sapporo, JAPAN 0608638
Phone: +81-11-706-7214; Fax: +81-11-706-7823
E-mail: toshimatsukawa@med.hokudai.ac.jp

Supplemental materials

Supplemental Table 1. Primer sequences for detection of *NUP98* fusion transcripts

primer	sequence (5'-3')
***NUP98* fusion F**	TCTTGGTACAGGAGCCTTTG
***NSD1* fusion R**	TCCAAAAGCCACTTGCTTGGC
***HOXA9* fusionR**	CAGTTCCAGGGTCTGGTGTT
***DDX10* fusion R**	TTTGCTGCAGCTCACAGACTATGT
***PMX1* fusion R**	CTGGCTGCTATTGAAGGTTGTC
***RARG* fusion R**	TGGGTCCGGTTCAGGGTCAGC

Supplemental Table 2. Primer sequences used for Sanger sequencing of *WT1* exons 7 and 9

primer	sequence (5'-3')
***WT1* ex7F**	TACTCCAGTGCTCACTCTCCC
***WT1* ex7R**	AGCTCTTGAACCATGTTTGCC
***WT1* ex9F**	ACTGTGCCCACATTGTTAGG
***WT1* ex9R**	CCCTCTCATCACAATTTCATTCC

Supplemental Table 3. Primer sequences used for RT-PCR analysis of *IL3RA* and *ACTB*

primer	sequence (5'-3')
***IL3RA*-F**	GGTGCGGAGAATCTGACCTG
***IL3RA*-R**	GTACTGTTGACGCCTGTTGG
***ACTB*-F**	AGGCCGGCTTCGCGGGCGAC
***ACTB*-R**	CTCGGGAGCCACACGCAGCTC

Supplemental Table 4. Primer sequences used for cloning of *IL3RA* promoter fragments (−977 to +110, −331 to +110, −215 to +110, and −76 to +110) into firefly luciferase reporter vectors

primer	sequence (5'-3')
pGL3-*IL3RA* promoter (-977)-F	tcttacgcgtgctagcccgggAACCTCTCTCCCAGGTTCAAACT
pGL3-*IL3RA* promoter (-331)-F	tcttacgcgtgctagcccgggACGCCTCCAAGGCTGAATTTACTA
pGL3-*IL3RA* promoter (-215)-F	tcttacgcgtgctagcccgggCGGGAACATGATAATTTTCAAAGA
pGL3-*IL3RA* promoter (-76)-F	tcttacgcgtgctagcccgggGATCCTTATTGGGTCTGAGTTTCAG
pGL3-*IL3RA* promoter -R	atcgcagatctcgagcccgggAACAGCCTTCGTGGTTCCAGT

Supplemental Table 5. Primer sequences used for ChIP-qPCR analysis of the *IL3RA* promoter (−76 to +110)

primer	sequence (5'-3')
***IL3RA* promoter (-76)-F**	GATCCTTATTGGGTCTGAGTTTCAG
***IL3RA* promoter -R**	AACAGCCTTCGTGGTTCCAGT

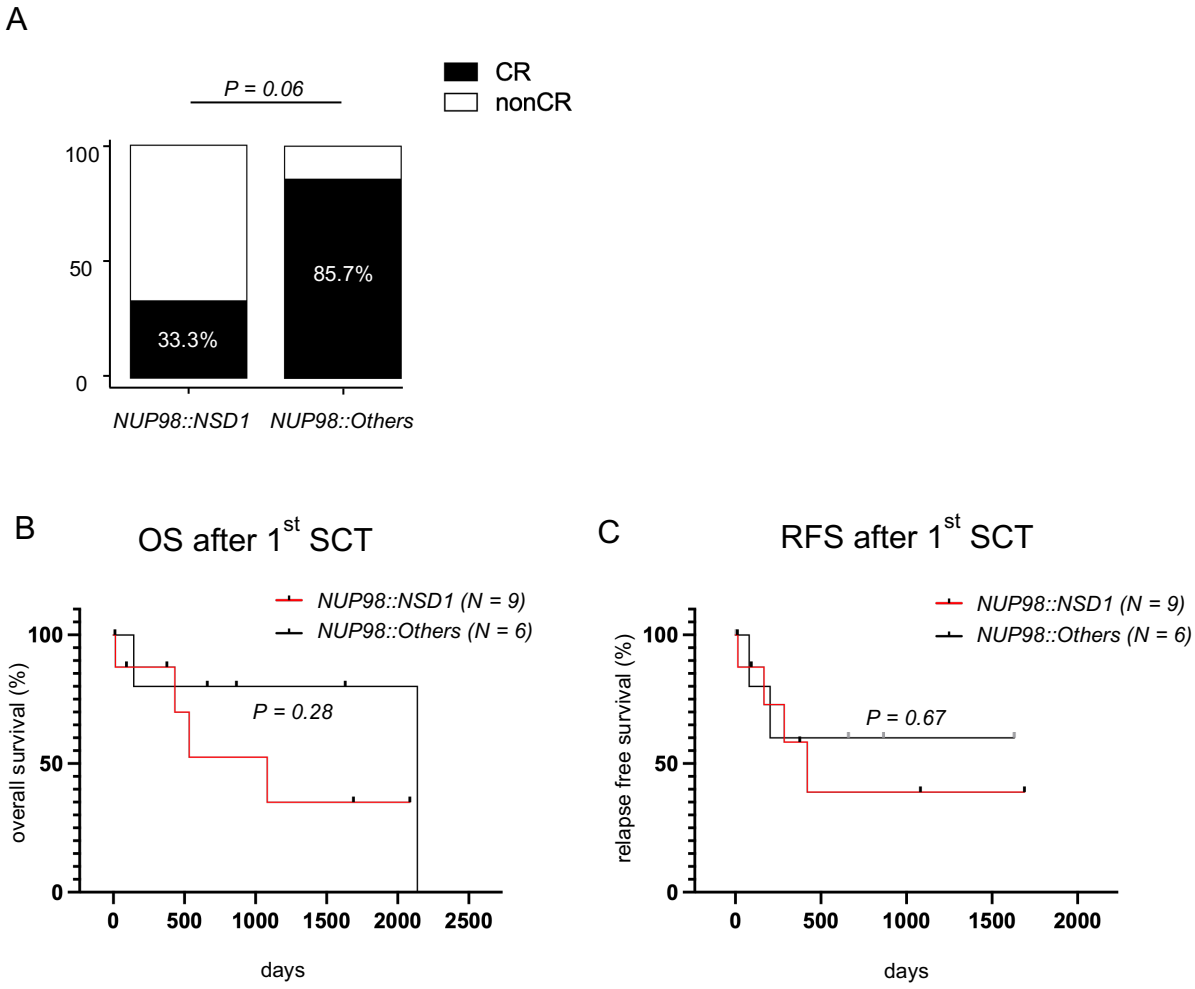

Supplemental Figure 1. Complete remission rate and post-transplant survival outcomes according to *NUP98* fusion subtype

(A) Stacked bars show the proportion of patients achieving complete remission (CR; black) or not achieving CR (nonCR; white) after induction therapy in the *NUP98::NSD1* group (4/12; 33.3%) and the *NUP98*::Others group (6/7; 85.7%). (B, C) Kaplan–Meier curves showing survival outcomes measured from the time of the first allogeneic stem cell transplantation (SCT). (B) Overall survival (OS) after first SCT in patients with *NUP98::NSD1* (N = 9) and those with other *NUP98* fusions (N = 6). (C) Relapse-free survival (RFS) after first SCT in patients with *NUP98::NSD1* (N = 9) and those with other *NUP98* fusions (N = 6).

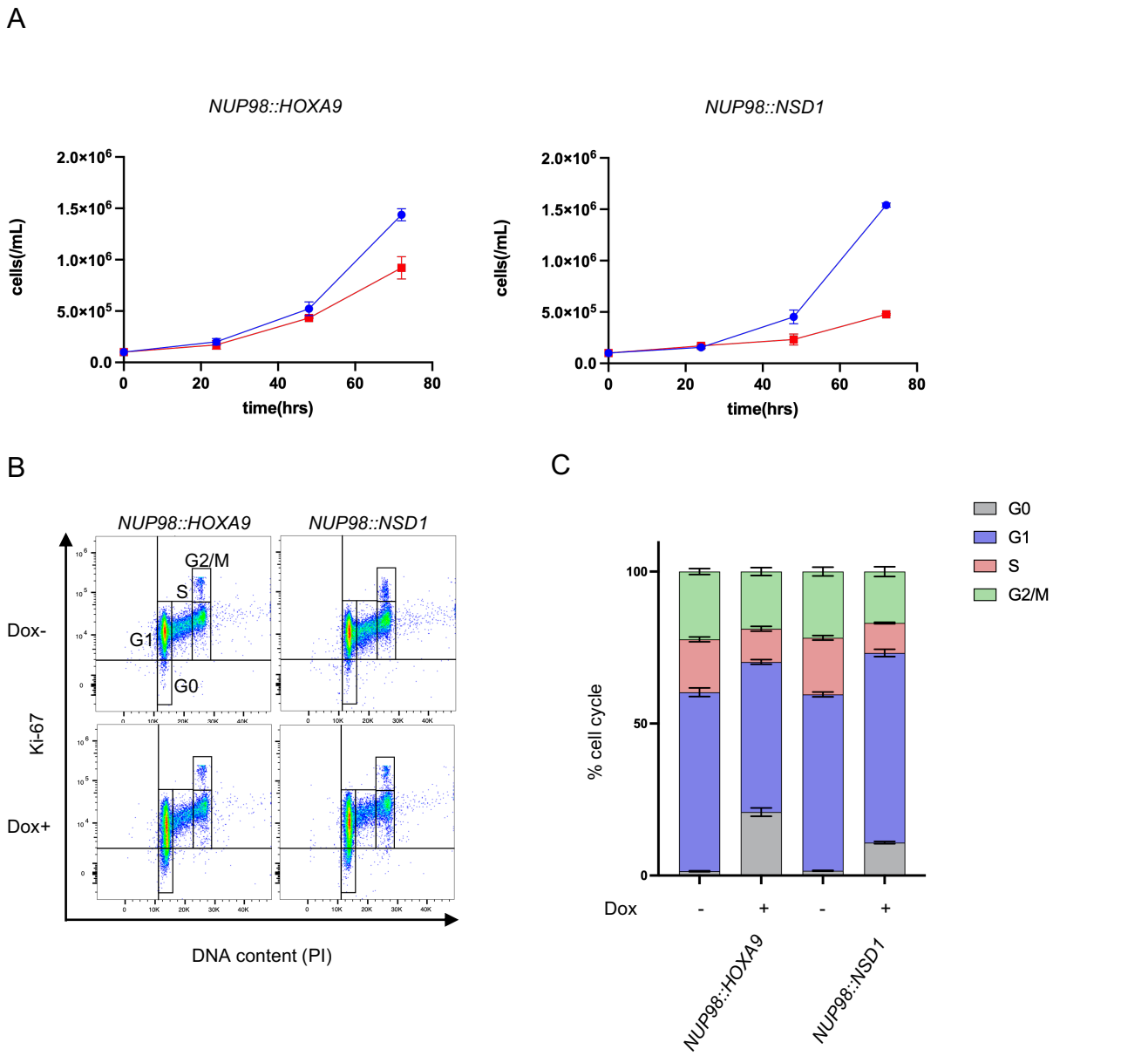
A
NUP98::HOXA9
NUP98::NSD1
cells(/mL)
time(hrs)
B
NUP98::HOXA9
NUP98::NSD1
Dox-
Dox+
Ki-67
G2/M
S
G1
G0
DNA content (PI)
C
G0
G1
S
G2/M
% cell cycle
Dox
NUP98::HOXA9
NUP98::NSD1
D
IDR
DNR
AraC
Dox-
Dox+
IC50 µM:
Dox- 0.29 / Dox+ 0.25
P = 0.79
Dox- 0.052 / Dox+ 0.14
P = 0.0002
Dox- 0.13 / Dox+ 0.11
P = 0.14
NUP98::HOXA9
relative viability vs DMSO
Dox- 0.31/ Dox+ 1.20
P < 0.0001
Dox- 0.052 / Dox+ 0.19
P < 0.0001
Dox- 0.12 / Dox+ 1.1
P < 0.0001
NUP98::NSD1

Supplemental Figure 2. *NUP98::HOXA9* and *NUP98::NSD1* regulate cell growth, cell-cycle progression, and drug responses in K562 cells

The effects of *NUP98::HOXA9* and *NUP98::NSD1* expression on cell growth, cell-cycle progression, and drug responses were additionally evaluated in K562 cells.

(A) Growth curves of *NUP98::HOXA9* and *NUP98::NSD1* cells cultured with or without doxycycline (Dox). (B) Cell-cycle analysis by Ki-67 and propidium iodide (PI) staining. (C) Quantification of cells in G0, G1, S, and G2/M phases. (D) Cell viability and drug response assays in inducible NUP98::HOXA9 or NUP98::NSD1 cells treated with the indicated concentrations of idarubicin (IDR), daunorubicin (DNR), or cytarabine (AraC) in the presence or absence of Dox. Cell viability is shown as a percentage of DMSO-treated controls.

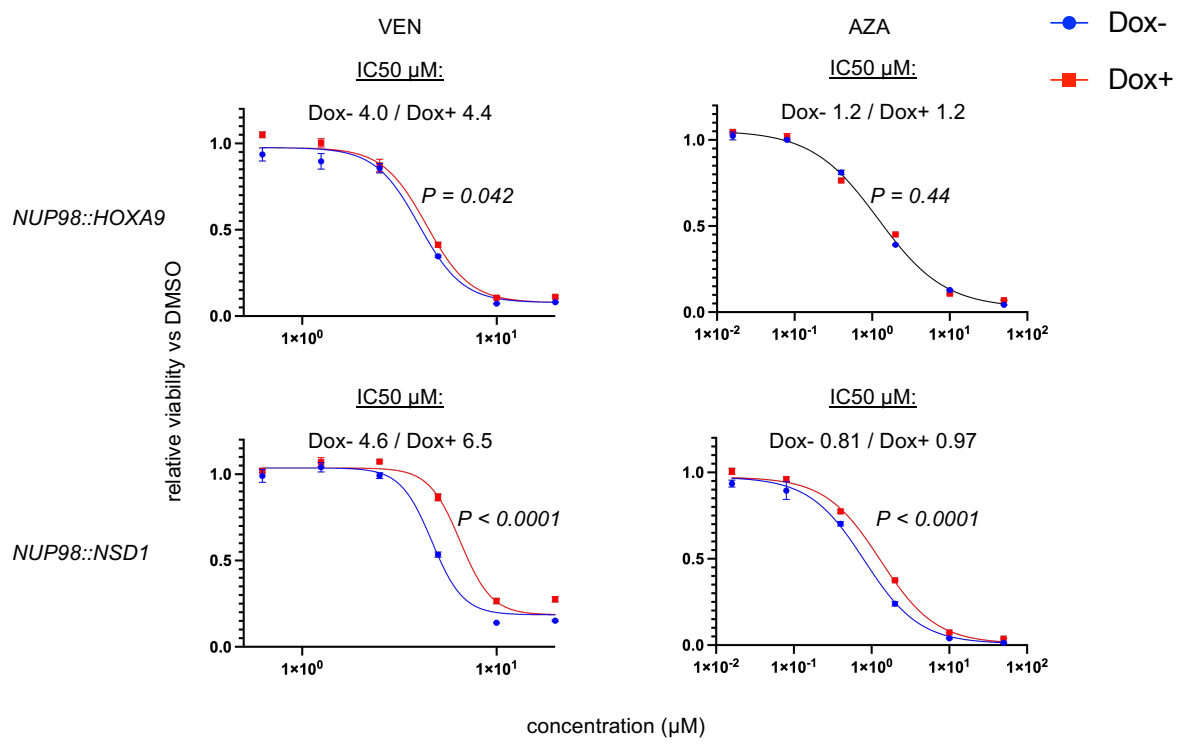

Supplemental Figure 3. Sensitivity to venetoclax and azacitidine in inducible *NUP98* fusion cells

Cell viability and drug response assays in inducible *NUP98::HOXA9* or *NUP98::NSD1* cells treated with the indicated concentrations of venetoclax (VEN) or azacitidine (AZA) in the presence or absence of Dox. Cell viability is shown as a percentage of DMSO-treated controls. Data are representative of 3 independent experiments.

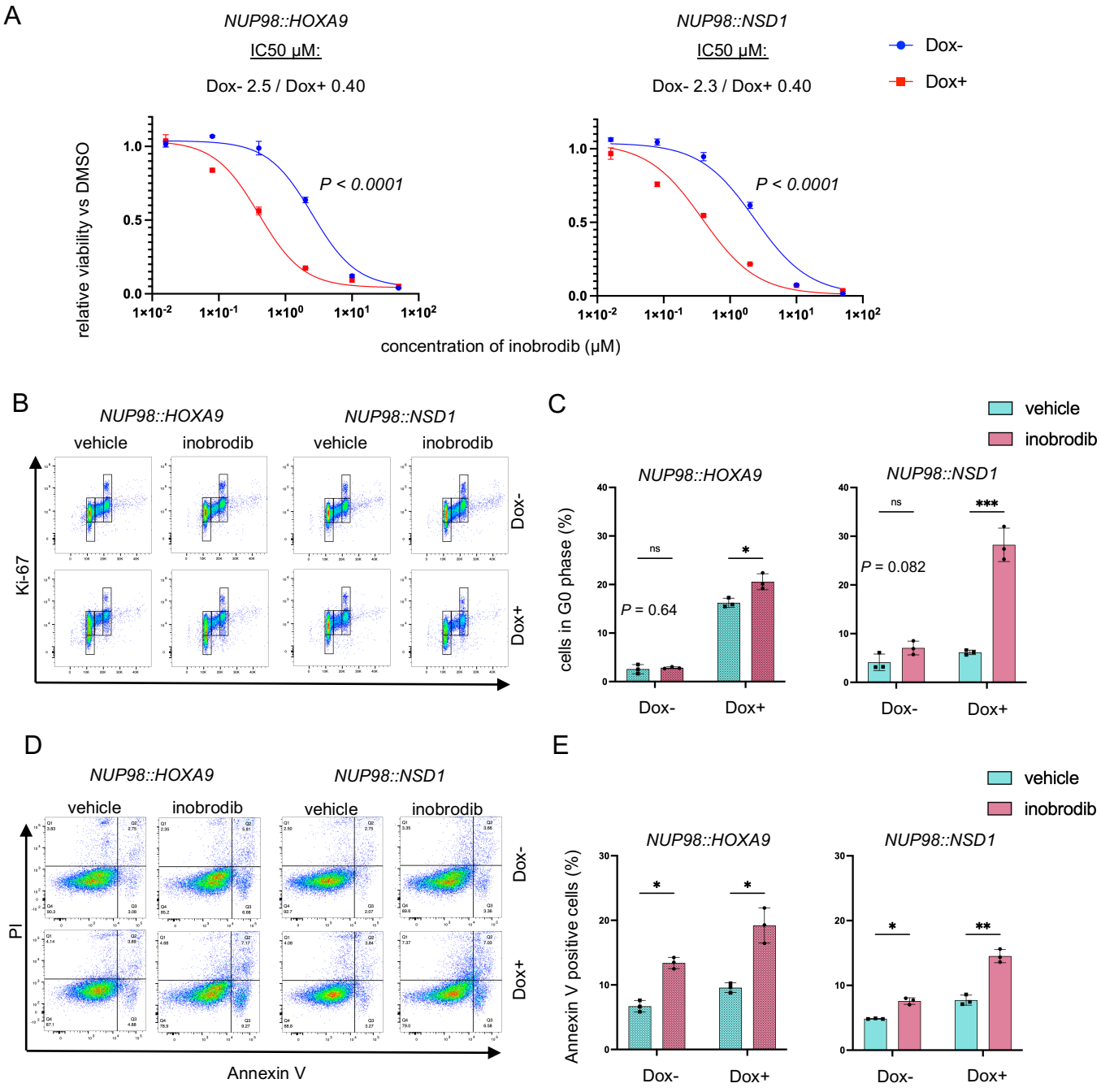

Supplemental Figure 4. Effects of inobrodib on cell viability, cell-cycle distribution, and apoptosis in inducible *NUP98* fusion cells

(A) Dose–response curves of *NUP98::HOXA9* (left panel) and *NUP98::NSD1* (right panel) cells treated with the EP300/CBP inhibitor inobrodib. Viability is shown as a percentage of DMSO-treated controls. (B) Cell-cycle analysis following treatment with vehicle or inobrodib in the presence or absence of doxycycline (Dox). Gates indicate the G0 phase defined by low/negative Ki-67 with 2N DNA content. (C) Quantification of the percentage of cells in the G0 phase under the indicated conditions. Statistical comparisons were performed between vehicle and inobrodib within each Dox condition. *P* values are indicated (*$P < 0.05$; **$P < 0.001$; ns, not significant). (D) Flow cytometric analysis of apoptosis by Annexin V and PI staining. (E) Quantification of the Annexin V–positive cells.

Supplemental methods

Patients, molecular screening, and ethics

Clinical samples were collected from patients diagnosed with AML between May 2016 and December 2025 at participating HLN institutions. HLN is a multicenter prospective cohort analyzing specimens from newly diagnosed AML cases at centers affiliated with the North Japan Hematology Study Group.[1, 2] AML diagnosis was established according to the 2022 World Health Organization classification, with retrospective reclassification of cases diagnosed before its publication as necessary. [3]

A tiered molecular screening strategy was used to identify *NUP98* rearrangements. Among patients diagnosed with AML, cases harboring other recurrent cytogenetic abnormalities such as acute promyelocytic leukemia (APL) and core-binding factor (CBF) leukemia were excluded from molecular screening. Because *NUP98::NSD1* is strongly associated with *FLT3*-ITD, [4, 5] AML cases positive for *FLT3*-ITD were preferentially screened for *NUP98::NSD1* fusion transcripts by reverse transcription PCR (RT-PCR) using primers designed on the basis of previously reported *NUP98::NSD1* fusion junctions. [6, 7] The identity of amplified products was confirmed by Sanger sequencing. *FLT3*-ITD status was determined by PCR-based fragment analysis according to standard clinical diagnostic procedures. For *NUP98* rearrangements involving fusion partners other than *NSD1*, cases with cytogenetic abnormalities suggestive of *NUP98* involvement were first identified by conventional karyotyping; candidate fusion transcripts were then evaluated by RT-PCR using partner-specific primers followed by Sanger sequencing. [8–10] The present cohort included six previously reported patients with NUP98::NSD1. [11]

This study was conducted in accordance with the Declaration of Helsinki and approved by the institutional review board of Hokkaido University Hospital(#015-0344). Primer sequences are listed in supplemental Table 1.

Targeted mutation profiling and *WT1* sequencing

Diagnostic genomic DNA was extracted from bone marrow aspirates or peripheral blood samples collected at initial presentation. Amplicon-based deep sequencing was performed using a compact AML panel covering mutation hotspots in 18 genes: *TP53, RUNX1, NPM1, FLT3, IDH1, IDH2, DNMT3A, ASXL1, EZH2, KRAS, NRAS, PTPN11, CBL, CEBPA, SF3B1, U2AF1, KIT,* and *BCOR*. Multiplex PCR amplicons were deep-sequenced on the MiSeq system (Illumina, San Diego, CA) at the Research Institute for Microbial Diseases, Osaka University (Osaka, Japan). Variants were retained for downstream analyses if coverage was ≥100× and VAF was >5%. Synonymous variants and known germline polymorphisms, including single-nucleotide polymorphisms, were excluded. The remaining variants were classified as mutations.

Because *WT1* was not included in the compact panel, *WT1* exons 7 and 9 were amplified from diagnostic genomic DNA and analyzed by Sanger sequencing. Primer sequences are listed in supplemental Table 2.

Cell lines and culture conditions

TF-1 cells were obtained from the American Type Culture Collection (ATCC, Manassas, VA, USA; CRL-2003) and maintained in RPMI-1640 supplemented with 10% fetal bovine serum (FBS), 1% penicillin–streptomycin (PS), and 2 ng/mL recombinant human granulocyte-macrophage colony-stimulating factor (GM-CSF) at 37°C in 5% CO_2. K562 cells were obtained from the JCRB Cell Bank (Osaka, Japan;

JCRB0019) and maintained in RPMI-1640 supplemented with 10% FBS and 1% PS at 37°C in 5% CO_2. HEK293T cells were obtained from the JCRB Cell Bank and maintained in Dulbecco's modified Eagle's medium (DMEM) supplemented with 10% FBS and 1% PS at 37°C in 5% CO_2.

Generation of doxycycline-inducible *NUP98* fusion models

NUP98::HOXA9 and *NUP98::NSD1* cDNA constructs were cloned into a piggyBac transposon vector containing a TRE promoter and a 3×FLAG tag. The rtTA3 cassette was co-expressed via an IRES sequence. TF-1 and K562 cells were nucleofected with the piggyBac transposon vector and a hyperactive piggyBac transposase vector using the 4D-Nucleofector™ System (Lonza, Basel, Switzerland) according to the manufacturer's instructions. Stable clones were selected with puromycin (1 μg/mL). Doxycycline (100 ng/mL) was used to induce fusion protein expression. After puromycin selection, polyclonal resistant cells were subjected to limiting dilution in 96-well plates to isolate single-cell–derived clones. Individual colonies were expanded, and three independent clones per construct were established for downstream analyses. For HEK293T cells, the same piggyBac vector design was used, and cells were transfected with the transposon and transposase vectors using Lipofectamine 2000 (Thermo Fisher Scientific, Waltham, MA, USA), followed by puromycin selection to establish Dox-inducible models.

Immunoblotting

Whole-cell lysates were prepared 24 h after treatment with doxycycline or vehicle. Briefly, 5×10^5 cells were resuspended in 100 μL of RIPA buffer (Nacalai Tesque, Kyoto, Japan) supplemented with Protease Inhibitor Cocktail Set I (FUJIFILM Wako Pure Chemical Corporation, Osaka, Japan) and Phosphatase Inhibitor Cocktail (Nacalai Tesque), incubated on ice for 15 min, and centrifuged at 10,000 × g for 10 min at 4°C. The resulting supernatants were collected as whole-cell lysates, mixed with 4× Laemmli Sample Buffer (Bio-Rad Laboratories, Hercules, CA, USA; Cat# 1610747), and boiled at 98°C for 5 min. Equivalent volumes of lysates were separated on Mini-PROTEAN TGX gels (Bio-Rad Laboratories; Cat# 4561086) and transferred to PVDF membranes using a Trans-Blot Turbo Transfer Pack (Bio-Rad Laboratories; Cat# 1704156). Membranes were blocked with PhosphoBLOCKER™ Blocking Reagent (Cell Biolabs, San Diego, CA, USA; Cat# AKR-104) for 1 h at room temperature, incubated with primary antibodies overnight at 4°C, and then with the appropriate HRP-conjugated secondary antibodies diluted 1:5000 for 1 h at room temperature. Protein expression was analyzed using anti-NUP98 (rat monoclonal antibody, clone 2H10; Santa Cruz Biotechnology, Dallas, TX, USA; Cat# sc-101546) and anti-β-actin (mouse monoclonal antibody; Sigma-Aldrich, St. Louis, MO, USA; Cat# A1978) antibodies. Secondary antibodies included rabbit anti-mouse IgG H&L (Abcam, Cambridge, UK; Cat# ab6728), anti-rabbit IgG, HRP-linked antibody (Cell Signaling Technology; Cat# 7074), and anti-rat IgG (H+L), HRP-conjugated antibody (Abcam; Cat# ab205720). Signals were detected using Amersham™ ECL™ Select Western Blotting Detection Reagent (Cytiva, Marlborough, MA, USA; Cat# RPN2235) and visualized with a ChemiDoc imaging system (Bio-Rad Laboratories). HEK293T cells transiently transfected with the corresponding NUP98 fusion construct were used as positive controls, and parental TF-1 cells were used as negative controls.

Subcellular fractionation

Cytoplasmic and nuclear fractions were prepared using the NE-PER™ Nuclear and Cytoplasmic Extraction Reagents (Thermo Fisher Scientific, Waltham, MA, USA) according to the manufacturer's instructions. The resulting fractions were analyzed by immunoblotting to assess the subcellular distribution of NUP98 fusion proteins.

Immunofluorescence

TF-1 cells were treated with doxycycline or vehicle for 24h, cytospun onto glass slides, fixed with 4% paraformaldehyde for 10 min at room temperature, and then treated with pre-chilled methanol at −20°C for 10 min. After three washes with PBS, cells were blocked with 1% bovine serum albumin for 30 min at room temperature and incubated with anti-NUP98 antibody (rat monoclonal, clone 2H10; Santa Cruz Biotechnology, Dallas, TX, USA; Cat# sc-101546; 1:100) for 1 h at room temperature. After three 5-min washes with PBS, cells were incubated with goat anti-rat IgG H&L (Alexa Fluor 488) secondary antibody (Abcam, Cambridge, UK; Cat# ab150157; 1:500) for 1 h in the dark. Cells were washed three times with PBS, counterstained with Hoechst 33258 solution (1:1000) for 1 min, washed once with PBS, mounted with coverslips, and examined using a BZ-X810 fluorescence microscope (Keyence, Osaka, Japan).

Cell viability and drug response assays

Cell viability was assessed using Cell Counting Kit-8 (CCK-8; Dojindo, Kumamoto, Japan). Cells were pretreated with Dox or vehicle for 24 h and then seeded at 3,000 cells per well in 96-well plates. Anticancer agents were added at the indicated concentrations and cells were incubated for an additional 48 h. CCK-8 reagent (10 μL) was added to each well, and incubated at 37℃ for 2 h. Absorbance at 450 nm was measured using a GloMax® Multi Detection System (Promega, Madison, WI, USA). Each condition was performed in technical triplicate wells. Background absorbance was subtracted using blank wells containing medium and CCK-8 reagent only. Viability was normalized to vehicle-treated controls and expressed as percent of control. Dose–response curves were fitted using a four-parameter logistic model in GraphPad Prism. IC50 values were compared between groups by global nonlinear regression with shared top/bottom and Hill slope and group-specific IC50, using an extra sum-of-squares F test. Drugs tested included idarubicin (IDR), daunorubicin (DNR), cytarabine (AraC), venetoclax (VEN), azacitidine (AZA), and inobrodib.

Cell-cycle analysis

Cell-cycle distribution was analyzed by Ki-67 and propidium iodide (PI) staining. Cells were harvested, washed with PBS, and fixed in 70% ethanol at −20°C overnight. After washing, cells were incubated with RNase A (100 μg/mL) and stained with PI (50 μg/mL) for 30 min at room temperature in the dark. For Ki-67 staining, fixed cells were incubated with anti-Ki-67 antibody (BioLegend, San Diego, CA, USA; Cat# 350514, RRID:AB_10959327). Data were acquired on a FACSCanto™ II flow cytometer (BD Biosciences, San Jose, CA, USA). Doublets were excluded by forward scatter height versus area gating. Cell-cycle phases (G0, G1, S, and G2/M) were quantified using FlowJo software based on DNA content and Ki-67 expression.

Apoptosis assay

Apoptosis was assessed using APC-Annexin V (BD Pharmingen™, San Diego, CA, USA) and PI staining. Cells were harvested, washed twice with cold PBS, and resuspended in Annexin V binding buffer (BD Pharmingen™). Cells were incubated with APC-Annexin V and PI for 15 min at room temperature in the dark. Samples were analyzed on a FACSCanto™ II flow cytometer (BD Biosciences). Doublets were excluded by forward scatter height versus area gating. Early apoptotic cells were defined as Annexin V–positive/PI-negative, and late apoptotic or necrotic cells as Annexin V–positive/PI-positive. Total apoptosis was calculated as the sum of early and late apoptotic cells.

RNA sequencing and differential expression analysis

Total RNA was extracted using the RNeasy Mini Kit (QIAGEN, Hilden, Germany). Poly(A)-selected, strand-specific RNA sequencing libraries were prepared using the NEBNext Poly(A) mRNA Magnetic Isolation Module and the NEBNext Ultra II Directional RNA Library Prep Kit (New England Biolabs, Ipswich, MA, USA). Sequencing was performed by Rhelixa, Inc. (Tokyo, Japan) on an Illumina NovaSeq X Plus platform to generate 150-bp paired-end reads, yielding an average of approximately 40 million read pairs per sample. Raw sequencing reads were assessed for quality using FastQC (v0.12.1). Adapter sequences and low-quality bases were trimmed using Trimmomatic (v0.38) [12] with the following parameters: ILLUMINACLIP:2:30:10, LEADING:20, TRAILING:20, SLIDINGWINDOW:4:15, and MINLEN:36. Trimmed reads were aligned to the human reference genome (GRCh38) using HISAT2 (v2.1.0). [13] Gene-level read counts were quantified using featureCounts (v1.6.3) [14] based on GTF gene annotations. Differential expression analysis was performed using DESeq2 (v1.24.0) [15] with RLE normalization. Genes with an adjusted P value <0.05 and an absolute log2 fold change >1 were considered differentially expressed. RNA sequencing was performed after 24 h of Dox treatment using three independent TF-1 clones per construct.

Flow cytometry

Flow cytometric analysis was performed using a FACSCanto™ II flow cytometer (BD Biosciences), and data were analyzed with FlowJo software. Cells were washed and resuspended in FACS buffer (PBS containing 0.5% bovine serum albumin and 2 mM EDTA), then stained with PE-conjugated anti-human CD123 antibody (BioLegend, Cat# 396604) at a 1:100 dilution for 30 min at 4°C in the dark. After washing, samples were acquired on the flow cytometer. Unstained cells were used as controls. Data were gated on FSC/SSC to exclude debris and subsequently on singlets. CD123 expression was assessed as both mean fluorescence intensity (MFI) and the percentage of positive cells.

RT-qPCR

Total RNA was extracted using the RNeasy Mini Kit (QIAGEN, Hilden, Germany). cDNA was synthesized using the SuperScript® III First-Strand Synthesis System (Invitrogen, Thermo Fisher Scientific, Waltham, MA, USA). RT-qPCR was performed using SYBR™ Green qPCR Master Mix (Thermo Fisher Scientific; Cat# A66732) on a CFX96 Real-Time PCR Detection System (Bio-Rad Laboratories, Hercules, CA, USA). Relative expression levels were normalized to ACTB using the ΔΔCt method.

Luciferase reporter assays

Luciferase reporter assays were performed as previously described with minor modifications. [16] IL3RA promoter fragments (−977 to +110 and truncated variants) were cloned into a pGL4 luciferase reporter vector. HEK293T cells engineered for Dox-inducible expression of NUP98::HOXA9 or NUP98::NSD1 were seeded in 24-well plates and co-transfected with the indicated firefly luciferase reporter constructs and a Renilla control plasmid using Lipofectamine 2000 (Thermo Fisher Scientific, Waltham, MA, USA). At 24 h post-transfection, Dox was added at 100 ng/mL to induce fusion expression, and firefly and Renilla luciferase activities were measured 24 h later using the Dual-Luciferase Reporter Assay System (Promega, Madison, WI, USA) and a GloMax® Multi Detection System according to the manufacturer's instructions. Firefly luciferase activity was normalized to Renilla luciferase activity to control for transfection efficiency. Each condition was analyzed in technical triplicate wells. Primers used to generate the luciferase constructs are listed in supplemental Table 4.

Chromatin immunoprecipitation (ChIP)-qPCR

ChIP-qPCR was performed in Dox-inducible TF-1 cells expressing *NUP98::HOXA9* or *NUP98::NSD1* in the presence or absence of Dox. Chromatin immunoprecipitation was performed using the SimpleChIP® Enzymatic Chromatin IP Kit (Cell Signaling Technology, Danvers, MA, USA) according to the manufacturer's instructions. Cells were cross-linked with 1% formaldehyde at room temperature and quenched with glycine. Cells were lysed, and cross-linked chromatin was enzymatically digested and sonicated to generate DNA fragments averaging ~300–1,500 bp. Chromatin was immunoprecipitated with antibodies against FLAG (Cell Signaling Technology; Cat# 14793), H3K27ac (Cell Signaling Technology; Cat# 8173S), or H3K27me3 (Cell Signaling Technology; Cat# 9722S). Normal rabbit IgG was used as a negative control. Purified DNA was analyzed by qPCR using primers spanning the *IL3RA* proximal promoter region (−76 to +110 relative to the transcription start site). ChIP enrichment was calculated as percent input. Primer sequences are listed in supplemental Table 5.

Statistical analysis

Data from the in vitro experiments are presented as mean ± standard deviation (SD) from at least three independent experiments unless otherwise stated. Dose-response curves were analyzed using a four-parameter logistic model, and IC50 values were compared using an extra sum of squares F-test. Comparisons between two groups were performed using Welch's t-test, and multiple group comparisons were conducted using one-way ANOVA as appropriate. The OS was defined as the time from diagnosis to death from any cause or to the last follow-up. The EFS was defined as the time from diagnosis to treatment failure, relapse, or death from any cause, whichever occurred first. Relapse-free survival (RFS) was defined as the time from first complete remission to relapse or death from any cause. The median follow-up duration was estimated using the reverse Kaplan–Meier method. Survival curves were estimated using the Kaplan–Meier method and compared using the log-rank test. Categorical variables were compared using Fisher's exact test.

Supplemental References

1. Matsukawa T, Yoshida S, Onozawa M, et al (2026) Adverse karyotype amplifies risk in secondary acute myeloid leukemia (AML) and AML with myelodysplasia-related changes. Hematology 31:2628479. https://doi.org/10.1080/16078454.2026.2628479

2. Yoshida S, Onozawa M, Miyashita N, et al (2023) Clinical features of complex karyotype in newly diagnosed acute myeloid leukemia. Int J Hematol 117:544–552. https://doi.org/10.1007/s12185-022-03522-6

3. Khoury JD, Solary E, Abla O, et al (2022) The 5th edition of the World Health Organization Classification of Haematolymphoid Tumours: Myeloid and Histiocytic/Dendritic Neoplasms. Leukemia 36:1703–1719. https://doi.org/10.1038/s41375-022-01613-1

4. Ostronoff F, Othus M, Gerbing RB, et al (2014) NUP98/NSD1 and FLT3/ITD coexpression is more prevalent in younger AML patients and leads to induction failure: a COG and SWOG report. Blood 124:2400–2407. https://doi.org/10.1182/blood-2014-04-570929

5. Kivioja JL, Martí JML, Kumar A, et al (2018) Chimeric NUP98–NSD1 transcripts from the cryptic t(5;11)(q35.2;p15.4) in adult de novo acute myeloid leukemia. Leuk Lymphoma 59:725–732. https://doi.org/10.1080/10428194.2017.1357174

6. Akiki S, Dyer SA, Grimwade D, et al (2013) NUP98-NSD1 fusion in association with FLT3-ITD mutation identifies a prognostically relevant subgroup of pediatric acute myeloid leukemia patients suitable for monitoring by real time quantitative PCR. Genes, Chromosom Cancer 52:1053–1064. https://doi.org/10.1002/gcc.22100

7. Jaju RJ, Fidler C, Haas OA, et al (2001) A novel gene, NSD1, is fused to NUP98 in the t(5;11)(q35;p15.5) in de novo childhood acute myeloid leukemia. Blood 98:1264–1267. https://doi.org/10.1182/blood.v98.4.1264

8. Nakamura T, Largaespada DA, Lee MP, et al (1996) Fusion of the nucleoporin gene NUP98 to HOXA9 by the chromosome translocation t(7;11)(p15;p15) in human myeloid leukaemia. Nat Genet 12:154–158. https://doi.org/10.1038/ng0296-154

9. Arai Y, Hosoda F, Kobayashi H, et al (1997) The inv(11)(p15q22) chromosome translocation of de novo and therapy-related myeloid malignancies results in fusion of the nucleoporin gene, NUP98, with the putative RNA helicase gene, DDX10. Blood 89:3936–44

10. Nakamura T, Yamazaki Y, Hatano Y, Miura I (1999) NUP98 Is Fused to PMX1 Homeobox Gene in Human Acute Myelogenous Leukemia With Chromosome Translocation t(1;11)(q23;p15). Blood 94:741–747. https://doi.org/10.1182/blood.v94.2.741

11. Miyajima T, Onozawa M, Yoshida S, et al (2023) Clinical implications of NUP98::NSD1 fusion at diagnosis in adult FLT3-ITD positive AML. Eur J Haematol 111:620–627. https://doi.org/10.1111/ejh.14055

12. Bolger AM, Lohse M, Usadel B (2014) Trimmomatic: a flexible trimmer for Illumina sequence data. Bioinformatics 30:2114–2120. https://doi.org/10.1093/bioinformatics/btu170

13. Kim D, Langmead B, Salzberg SL (2015) HISAT: a fast spliced aligner with low memory requirements. Nat Methods 12:357–360. https://doi.org/10.1038/nmeth.3317

14. Liao Y, Smyth GK, Shi W (2014) featureCounts: an efficient general purpose program for assigning sequence reads to genomic features. Bioinformatics 30:923–930. https://doi.org/10.1093/bioinformatics/btt656

15. Love MI, Huber W, Anders S (2014) Moderated estimation of fold change and dispersion for RNA-seq data with DESeq2. Genome Biol 15:550. https://doi.org/10.1186/s13059-014-0550-8

16. Hou Z, Ren Y, Zhang X, et al (2024) EP300-ZNF384 transactivates IL3RA to promote the progression of B-cell acute lymphoblastic leukemia. Cell Commun Signal 22:211. https://doi.org/10.1186/s12964-024-01596-9